

EXTERNALLY BONDED FBG STRAIN SENSORS FOR STRUCTURAL HEALTH MONITORING OF MARINE HYDROKINETIC STRUCTURES

Michael Schuster
 Montana State University
 Bozeman, MT

Nathan Fritz
 Montana State University
 Bozeman, MT

Jarlath McEntee
 Ocean Renewable Power Company
 Portland, ME

Tom Graver
 Micron Optics Inc.
 Atlanta, GA

Mark Rumsey
 Sandia National Laboratories
 Albuquerque, ME

Bernadette Hernandez-Sanchez
 Sandia National Laboratories
 Albuquerque, NM

David Miller
 Montana State University
 Bozeman, MT

Erick Johnson¹
 Montana State University
 Bozeman, MT

¹Corresponding author: erick.johnson@me.montana.edu

ABSTRACT

In order to reduce operations and maintenance costs, mitigate failures, and improve capacity factor, structural health-monitoring systems can provide key information to improve management of marine hydrokinetic devices. While present systems include instrumentation to measure power output, few adequately monitor mechanical loads and structural response, which are equally important for determining device performance and integrity. Fiber optic fiber Bragg grating (FBG) sensors could prove to be a reliable and unobtrusive measurement tool for marine power; however, externally adhered FBGs have not been extensively on submerged, dynamic structures. To investigate the bond integrity between sensor and structure of a kinetic system, FBG strain sensors were tested in dry and environmentally soaked conditions under both static and fatigue loads. Composite coupons were strained in a fatigue testing system and monitored. Dry results demonstrated very high correlation and response from the FBG sensors, up to coupon failure. The environmentally soaked samples and sensors were subject to many modes of failure and verified the developer recommendation to not externally adhere the FBG strain sensors without additional mechanical and environmental protections.

INTRODUCTION

Operations and maintenance (O&M) costs for marine hydrokinetic (MHK) devices are anticipated to be significantly higher than those currently seen in the wind industry. This is due to their limited accessibility and the expense of the equipment required for servicing them. Even when accounting for a scaled increase in a deployment, O&M costs are expected to be the second largest expense, behind device production [1, 2]. Also, unlike stationary platforms and ships, MHK devices are, by design, dynamic structures and will require sensors and sensor-integration appropriate for these systems and environments. Without regular attention, materials, adhesives, and coatings in water degrade over extended periods of time, increasing the modes of failure. Successful testing and commercial scale deployments of MHK devices will rely, in part, on understanding the changes composite materials undergo when submerged in seawater and their bulk response as part of a dynamic system. In a wet environment, porosity, inherent to any composite matrix, will absorb water by Fickian Diffusion and has been shown to affect the mechanical properties of the laminate [3-7]. Water uptake also causes the laminate to swell and induce additional strain within the material. Environmental temperatures have been shown to influence the rate of water diffusion [8-10] and

biofouling has been shown to have detrimental effects on composite materials [11].

Without appropriate instrumentation and control, predetermined and regular inspections will be required for examination and repair, even if no service is necessary. And visual examination alone will not reveal sub-structure modes of failure. Furthermore, insufficient instrumentation could result in unexpected failure of the device, yielding little to no knowledge regarding the source and mode of failure. Seasonality and stochastic weather events will impact schedules and may preclude repairs for stretches of time, resulting in zero power production. However, consistent and detailed monitoring of MHK structural health would allow inspections to be scheduled when necessary. The potential for a failure could be detected in advance, the device taken offline or left in a limited operating state, and damages repaired before total failure of the structure/device. If a failure did occur, sensor behavior preceding the failure could be noted and used to prevent subsequent failures of other units.

A means of structural health monitoring will undoubtedly lead to more efficient operation of MHK devices. However, limited understanding of material and sensor response *in situ* [12-16] may result in false-positive failures; further increasing O&M expense. In lieu of electrically resistive sensors under water, fiber optic sensors provide an attractive method for long term structural health monitoring. Fiber-Bragg grating (FBG) strain sensors have found successful application in aerospace and wind energy technologies [17-19] and are a promising solution to provide effective data collection in the marine environment due to their size, material compatibility, accuracy, and reliability. FBG sensors are manufactured from fiber optic cables by inscribing a periodic pattern into the fiber core over a small gage section with a UV laser. The grating reflects a particular frequency of light back to the source interrogator to be measured. Provided they respond to different wavelengths, multiple FBGs can be connected in series on the same fiber. Operating as either a strain or temperature sensor, the fiber is strained mechanically (or thermally), changing the refraction and period of the inscription and thus the frequency of light reflected. This wavelength shift can be developed into a calculated mechanical strain [20].

While these sensors have been used extensively elsewhere, little work has been performed to characterize the best methods of incorporation of these sensors into dynamic,

composite structures that operate in a marine environment. Adhesion to the external surface of a structure will leave the sensor and bond exposed to the environment, even with a protective coating, over time. This method will additionally impact hydrodynamic performance. Bonding to an interior surface, when available, does not preclude environmental exposure, nor prevent fatigue failure of brittle adhesives. Moreover, this results in a smaller measured strain. Embedding sensors within the composite laminate is the most ideal method for strength and protection and is available only during manufacture or as a post-manufacture procedure. However, both approaches have a high probability of introducing structural defects, reducing the strength and lifespan of the structure. This study seeks to bracket FBG sensor effectiveness in the marine environment between ideal (dry) and long-term, environmentally exposed conditions. Coupon measurements will investigate: 1) the material properties of composite specimens that have been exposed to an MHK environment, and 2) the bond integrity of externally adhered fiber optic FBG sensors to these composite specimens. The method used for bonding the FBG sensors was *not* recommended by the developer for use in a marine environment, but chosen to represent the harshest environmental conditions possible.

EXPERIMENTAL SETUP

A test section of a marine hydrokinetic turbine foil, 1.2 m in span, was provided and cut into 60 test coupons, such that surface curvature effects were minimized while ensuring viable samples. A cross section of the foil can be seen in Figure 1. The foil was manufactured from an alternating layup of fiberglass and carbon fiber laminate plies using a vacuum bagging process that compresses the dry fabric before a resin matrix was injected. The thinner, high-pressure side was 7.5mm thick and the thicker, low-pressure side this was 10mm thick. The largest servo-hydraulic load frame available at MSU has a load capacity of 250kN and test samples had to be made small enough to statically fail under this load. Coupons, ideally sized and cut samples, were taken from both the low- and high-pressure sides to accommodate dry and soaked testing of 3 sensor types under static and fatigue loads, while also providing enough traveler coupons for additional comparison. Traveler coupons are control samples that undergo the same environmental exposure, but are not altered in any other way. The final coupon dimensions were 300mm long by 20mm wide

with thickness dependent on the surface selection. The samples were cut along the 0° fiber orientation (the span of the foil) to emulate the predominate bending load direction.

FBG Sensors and Attachment

Three FBG sensor families from Micron Optics Inc. were tested: uncoated and recoated variants of the os1100 and the packaged os3200. The os1100 sensors have a polyimide coating surrounding the fiber that provides additional environmental and mechanical protection, while aiding transfer of strain to the fiber core. When inscribing the FBG, the polyimide coating is removed and typically recoated after the FBG is inscribed. The recoated diameter is listed as being between 145-165 μm . Half of the os1100 sensors tested did not have a polyimide recoating over the sensor area. The os3200 is a packaged FBG sensor. A plastic casing protects the sensor and the fiber is sheathed in a 1 mm diameter braided cable. The casing provides significant protection to the sensor and ensures easy attachment to a surface.

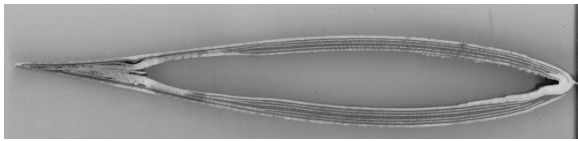


FIGURE 1: FOIL CROSS SECTION

The fiber Bragg grating strain gages were attached following the adhesion instructions supplied by MOI, but did not include the recommended additional mechanical and environmental protections. MOI recommends the fibers be integrated into the manufacturing process or that they be installed using a retrofit procedure that shields the sensors from direct contact with the marine environment. Neither was performed in these tests. These protective steps were omitted to investigate a worst-case scenario, aging of the samples, and environmental exposure on all coupon sides. Furthermore, composite MHK manufacturers may be hesitant to embed or retrofit sensors for fear of compromising the structural integrity of the composite layup. Additionally, water may penetrate a protective coating if damage is done to the hydrofoil by foreign objects or from cracks in the coating that may develop after the numerous cycles in the device's lifetime. This test setup should demonstrate the basic effects of seawater on these sensors and the results if they are not rigorously maintained and/or integrated into MHK devices.

It was necessary to adapt standard mounting procedures to mount the sensor on composites. The surface of every coupon was lightly sanded with P120 and P240 sandpaper, cleaned with acetone and alignment references were penciled onto the coupon. For the os1100 series sensors (both uncoated and recoated), small pools of Loctite 401 were placed on the surface of the future sensor location and, once dry, sanded flat with P120, P240, and P400 sandpaper. The surface was then cleaned with isopropyl alcohol. The sensors were placed under slight tension, aligned with the reference marks, and taped down at points approximately 2.5cm away from the FBG sensor. The FBG sensor was sprayed with Loctite Activator 7457 and 1 minute later, approximately two drops of Loctite 401 was spread over the sensor area. After an additional 10 minutes the tape was replaced with drops of Loctite 401 to act as strain relief.

The os3200 series FBG sensors were mounted according to mounting instructions available online [21]. All sensor types were cured at room temperature for a minimum of 24hrs before any measurements were taken.

Soak Process

The set of coupons to be soaked in salt water were placed tubs with the FBG connects passed through a hole in the lid and out of the water, as shown in Figure 2. ASTM standard D570 was used to simulate a marine environment and the tubs were placed in a furnace for five months at 50° to assist salt-water diffusion. This is within the operating range of both sensors [22, 23]. Mass and wavelength measurements were taken for every coupon before and after the soaking process. These measurements were also tracked for a set of representative coupons during the first month to determine the amount of water absorbed by the composite matrix and its effect on material strain.

Mechanical Testing

Mechanical testing was completed on an Instron 5882 servo-hydraulic load frame. Approximately 75 mm on both sides of each coupon was gripped with 10 MPa of pressure. Some strain was induced in the coupon when the grips were clamped down due to the slight curvature of the coupons. This strain was measured through an early test utilizing foil strain gages on both sides of the coupon and found to be minimal.



FIGURE 2: COUPONS IN SOAK TUBS

The static tests were run at an extension speed of 0.0254 mm/s in a ramped load until complete failure occurred. An extensometer was placed at the same location as the FBG to correlate strain readings from the interrogator. The temperature sensor was taped to each coupon during testing, the initial wavelength noted and strain readings zeroed. The interrogator was set to run at its max rate, 2 Hz, with sensors, peaks and events continuously monitored. A full spectral response was taken every minute in order to observe sensor degradation. Load and strain data from the Instron were recorded using a separate data acquisition system at a sample rate of 100 Hz.

TABLE 1: COUPON NUMBERS WITH CORRESPONDING TEST CONDITIONS

Test Matrix and Coupon Numbers				
Sensor	Static		Fatigue	
	Dry	Soaked	Dry	Soaked
none	2	32	17	47
	3	33	18	48
	41	42	56	57
1100c	4	34	19	49
	5	35	20	50
	6	36	21	51
1100u	8	38	23	53
	9	39	24	54
	10	40	25	55
3200	13	43	28	58
	14	44	29	59
	15	45	30	60

For fatigue tests, the maximum cyclic rate was limited to 1 Hz to avoid thermal effects affecting the results. With the interrogator running at 2 Hz, two values of strain could be recorded for each cycle. At each 1000 cycles the test was stopped

and 5 full cycles run at 0.02 Hz so the interrogator could record a full image of the strain. The test matrix detailing the sensor type and test condition to coupon number can be seen in Table 1. Three coupons were to be tested for each possible configuration.

RESULTS

The first month of the soak remained closely monitored, as described above, while no measurements were taken during the latter four months until prior to testing. Over the course of this time, the coupons gained, on average, 2.2% of their original mass with the representative coupons plotted in Figure 3. After five months, the average mass gain was up to 3.8% for all soaked coupons. Again, neither the sensors nor composite had protective coatings to mitigate environmental effects, as diffusion from the sides was not prevented.

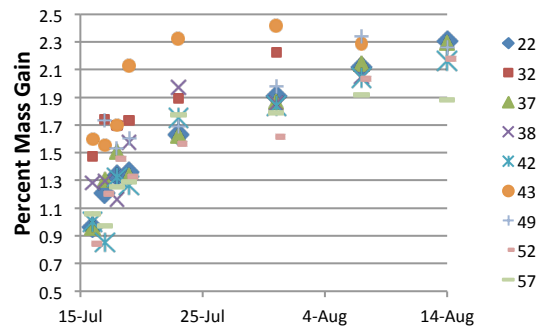


FIGURE 3: PERCENT MASS GAIN FOR SELECT COUPONS, 1 MONTH

While the FBG sensor connections were kept out of the salt-water, the braided sheathing was able to soak up salt-water along with the coupon. This would account for some noise in the mass gain values; however, the traveler coupons without any sensors gained a comparable mass during the soak, suggesting that the sheathing did not absorb a significant mass of salt-water. Since the uptake of salt-water will cause the coupon to swell, it was also of interest to note any wavelength shift. Figure 4 shows the percent wavelength change for the select coupons that were monitored closely throughout the month. From this figure it can be seen that there was some swelling that created a strain in the coupon material, however, the percent change overall was within measurement noise. As the strain readings were temperature dependent, a temperature correction was applied to the wavelength values.

Because the probe was not immersed in the salt-water tubs, but rather attached to the outside, there is some error in the temperature readings due to convection that affect the wavelength shift values.

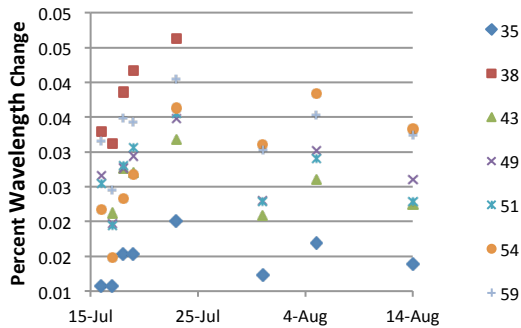


FIGURE 4: PERCENT CHANGE IN WAVELENGTH FOR SELECT COUPONS, 1 MONTH

Qualitative changes of the samples were also observed during the environmental soak. At the end of the one-month soak all sensors returned clean wavelength signals and the samples showed no visual degradation. After the one-month soak, the sensors were left undisturbed for the following four months until immediately prior to mechanical testing. When removed at that time, it was found that the condition of the sensors had degraded significantly. The protective polyimide coating surrounding the fiber had become very brittle. On almost all coupons, it had begun to split and peel away leaving the fiber exposed. The sensors were, in general, delicate and easily damaged, leading to lead wires failing at the strain relief points.

Upon connecting the sensors to the interrogator for a final wavelength measurement, five out of six uncoated os1100 sensors returned no peak, or the signal was severely degraded with competing peaks yielding unreliable readings. This effect was not seen in the recoated os1100 sensors (even after polyimide removal) or the os3200 sensors. The sensor areas were never directly exposed to the salt-water due to the Loctite adhesive holding the os1100 sensors in place, protecting the FBG, or the os3200 packaging.

Static Testing

The three FBG strain sensors performed well in the dry, static coupon tests and clearly established a baseline mode of failure. All of these sensors failed at strains greater than their 0.5%

manufacturer recommended strain limit, which is a common limit for fiber optic cables. As the peak wavelength response moved further from its original tuned wavelength, the peak did degrade, evident by a widening in wavelength and flattening in the power spectrum. However, this did not limit the default software settings from adequately capturing the principal wavelength. Failure of the sensor was characterized by a sudden loss of the tuned wavelength peak. The software often identified a new peak to return a strain value after failure, but by analyzing the spectral response it was clear that the returned value was erroneous. The spectral response of coupon 9 is shown in Figure 5, where the upper plot shows a healthy and well-defined peak while the lower plot is representative of a failed sensor.

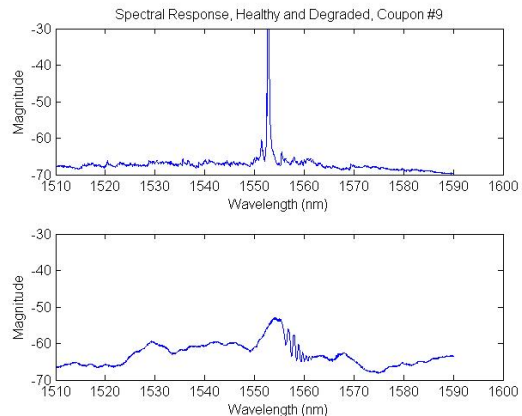


FIGURE 5: COMPARISON OF HEALTHY AND FAILED SENSOR SPECTRAL RESPONSE

The different sensor types did show a distinct trend in their strain at failure, which may be representative of the support from the protective packaging. This is shown in Figure 6. The os1100 sensors failed in tension prior to the coupon, but at a strain larger than the recommended maximum of 0.5%. The os3200 packaged sensors showed the greatest ability to strain with the coupon. These sensors were only damaged when energy release during coupon failure destroyed the bond. At no time did any of the sensors become detached from the coupons before coupon failure; nor was there delamination between the glass and carbon plies.

Also of interest was the accuracy of the FBG strain measurements throughout the mechanical testing. Figure 7 shows the strain readings from the extensometer and an uncoated os1100 FBG, sample 9, plotted against time. As seen, the strain readings correlate very well up until sensor

failure; however, the FBG jumps slightly in its reading over the course of time. This occurs as the sensor response begins to degrade and the software detects multiple, small wavelength peaks that each fit the peak definition criteria. Each could be selected as the true peak and the software determines the peak that best fits the given criteria, however incorrect it may be. It needs to be noted that the software does allow parameter calibration that could reduce the error in peak selection and that the peaks selected are very near the true strain. Also seen in Figure 7 is that the software does return a value after sensor failure though it is very much in error.

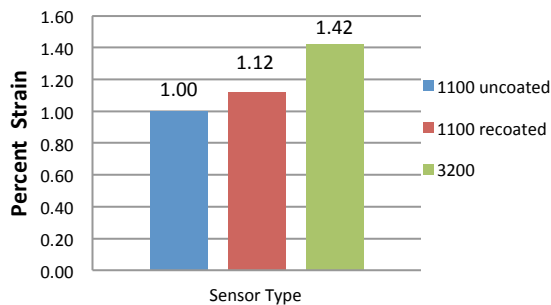


FIGURE 6: AVERAGE STRAIN AT SENSOR FAILURE FOR DRY, STATIC COUPONS

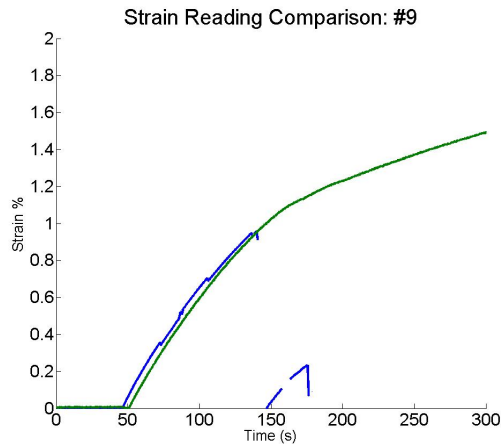


FIGURE 7: COMPARISON OF EXTENSOMETER AND FBG STRAIN USING EXTENSOMETER (GREEN) AND UNCOATED OS100 (BLUE)

Static mechanical testing of the dry coupons reinforced that the sample curvature may have introduced asymmetrical straining of the coupons when both sets of grips in the Instron were clamped down, however minor. As there was no dog-boning of the samples, and due to the high grip pressure required, the coupons often experienced grip failure. Grip failures are a result of the complex stress state that deviates from the

pure axial stress experienced in the test section of the coupon. As a result, the material reaches its strength limit in the grip area before the gage section. As the coupons in this study suffered from these effects, the strength and strain to failure values contain inherent error. However, data regarding sensor performance up until failure remains valid.

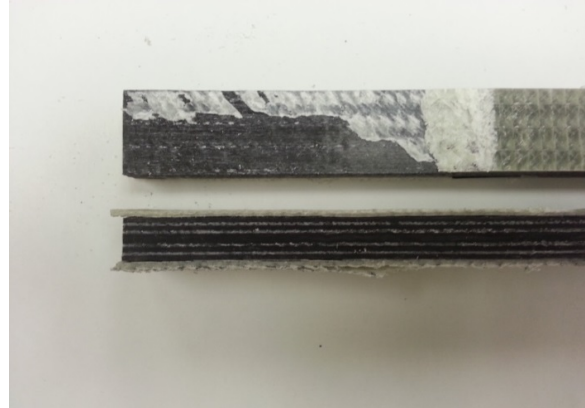


FIGURE 8: SOAKED COUPON WITH OUTER-GLASS SHEARING

Three baseline coupons, which did not have an FBG sensor attached, were the first soaked, static samples tested and could not be successfully tested to full failure. The outer glass plies, now saturated with salt-water, sheared away from the adjacent carbon layer, as seen in Figure 8. It is suspected insufficient resin infusion during manufacture may have contributed to a weak interlaminar bond between the glass and carbon. Air pockets between the plies were noted during initial inspection of the coupons. As a result of this mode of failure, accurate stress and strain values in the coupon were impossible to achieve through static testing. None of the three traveler coupons were able to reach 1% strain before the glass began to shear.

Even though accurate material data could no longer be collected, the sensors could still be tested. Again, the uncoated os1100 no longer returned viable signals. The recoated os1100 sensors were successfully tested to an average of 0.65% before signal degradation occurred. The os3200 sensors were tested, but the process of attaching the extensometer (which is held on with small rubber bands) damaged the three sensors and the wavelength peak could not be recovered. This did not occur during dry testing.

Fatigue Testing

Dry and environmentally-soaked coupons, with the recoated os1100 sensor, were tested using an

R-value of 0.1 to produce a maximum load near 0.75% strain, and based upon the dry, static test results. This resulted in maximum and minimum tensile loads of 28 kips and 2.8 kips, respectively, at a frequency of 1 Hz. Dry, fatigue tests demonstrated good agreement between the FBG sensors and the extensometer. Temperature compensated strain measurements for sample 20 are shown in Figure 9. The dry coupons failed at an average of 3,000 cycles and occurred earlier than would be expected for this layout. Similar carbon fiber laminates have been shown to strain statically to 1.5% and fail in the realm of one million cycles at 0.5% strain [24]. Fatigue failure consistently occurred within the grips. This is likely a result of the high grip pressures in conjunction with the curvature of the coupons and was not attributed to the shear between the outer glass and carbon layers, as seen in the wet, static tests. While this indicates error in failure loads, the performance of the FBG sensors may still be evaluated. For all of the dry samples, the coupons failed before the sensors and sensor bonds and provided clean output signals.

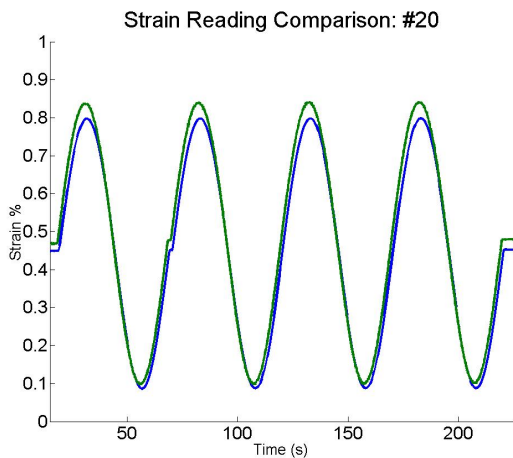


FIGURE 9: STRAIN RESPONSE FOR FATIGUE TEST OF SAMPLE 20 USING EXTENSOMETER (GREEN) AND RECOATED OS100 (BLUE)

Only a single soaked, recoated os1100 was tested in fatigue. The two other samples failed in the fiber cable after a final wavelength was measured, but prior to testing. Signal degradation was noted near peak strains (past the recommended maximum), but did not propagate through individual cycles. As with the dry samples, the coupon failed prior to the sensor. Up until failure, the FBG sensors performed well compared to the extensometer.

CONCLUSION

A comparison of fiber optic fiber Bragg grating strain sensors under ideal and long-term environmentally soaked conditions was performed in order to bound the performance of these sensors for marine hydrokinetic applications. Under dry, static and fatigue tests, all sensors were accurate, repeatable, and performed beyond their recommended maximum strains. After advanced aging in a salt-water bath, each FBG sensor family exhibited different modes of failure. The uncoated FBG sensors were unable to return a usable signal. The recoated FBG sensors appeared to be the most reliable and failed at strains lower than the ideal conditions, but still above the recommended maximum strain. The polyimide coating for both the uncoated and recoated sensors was not resistant to the environment and sloughed away from the fiber. Each of the packaged FBG sensors returned a viable wavelength prior to static testing, but became damaged through further handling, and the exact failure mode is unknown. The sensors were not environmentally protected using the developer recommendations in order to appropriately bracket the problem.

Up until failure, the FBG sensors performed well under dry and soaked conditions. The signals remained clean past the rated strain loads and did not degrade as a function of the cycle number. These sensors are small in size and more environmentally compatible than foil gages. As a result, fiber optic sensors should be considered for MHK applications. Appropriate selection of strain gages and placement will be highly dependent upon the expected device strains; however, material limitations are anticipated to maintain these at lower levels to achieve operational lifespans of more than a couple of years. External mounting of these sensors is not recommended for lifecycle measurements, they appear as if they will perform well for short measurement campaigns. Using fiber coatings and adhesives more appropriate for the marine environment will further improve reliability, but are unlikely to be sufficient at providing operational lifespan protection.

The mechanisms of sensor degradation while subject to environmental conditioning with salt-water need more investigation. Even as work progresses towards embedding the sensors into the hydrokinetic foil material, salt-water will penetrate the composite laminate, whether it be from damage or degradation of a protective coating, and this study has shown that the sensors

will be affected. Future experimental coupon tests should use dog-boned samples cut from a flat plate of representative material to reduce the required grip pressure and ensure material failure near the sensor location. This creates a well-defined gage section that will produce an accurate and repeatable failure under reduced tensile loads. Additionally, shorter aging times and protection methods should be investigated to more fully understand sensor lifespan. Incorporation of the sensors into the manufacturing processes and composite layup will also need to be considered. This provides a more reliable method of mechanical and environmental protection and given the results from the work performed above are certainly necessary. Due to fiber optic cables having the potential to introduce defects into the final composite laminate, their inclusion must be thoroughly researched, designed, and integrated.

ACKNOWLEDGEMENTS

This work was sponsored Sandia National Laboratories' Water Power Technology department and by the Department of Energies' Wind and Water Power Technologies Office. Sandia National Laboratories is a multi-program laboratory managed and operated by Sandia Corporation, a wholly owned subsidiary of Lockheed Martin Corporation, for the U.S. Department of Energy's National Nuclear Security Administration under contract DE-AC04-94AL85000.

REFERENCES

[1] Bull, D., Ochs, M. E., Laird, D. L., Boren, B., and Jepsen, R. A., 2013, "Technological Cost-Reduction Pathways for Point Absorber Wave Energy Converters in the Marine Hydrokinetic Environment," Sandia National Laboratories.
[2] Laird, D. L., Johnson, E. L., Ochs, M. E., and Boren, B., 2013, "Technological Cost-Reduction Pathways for Axial-Flow Turbines in the Marine Hydrokinetic Environment," Sandia National Laboratories.
[3] Chiou, P. L., and Bradley, W. L., 1997, "Seawater effects on strength and durability of glass/epoxy filament-wound tubes as revealed by acoustic emission analysis," *Journal of Composites Technology & Research*, 19(4), pp. 214-221.
[4] Gellert, E. P., and Turley, D. M., 1999, "Seawater immersion ageing of glass-fibre reinforced polymer laminates for marine applications,"

Composites Part a-Applied Science and Manufacturing, 30(11), pp. 1259-1265.

[5] Merah, N., Nizamuddin, S., Khan, Z., Al-Sulaiman, F., and Mehdi, M., 2010, "Effects of harsh weather and seawater on glass fiber reinforced epoxy composite," *Journal of Reinforced Plastics and Composites*, 29(20), pp. 3104-3110.

[6] Nogueira, P., Ramirez, C., Torres, A., Abad, M. J., Cano, J., Lopez, J., Lopez-Bueno, I., and Barral, L., 2001, "Effect of water sorption on the structure and mechanical properties of an epoxy resin system," *Journal of Applied Polymer Science*, 80(1), pp. 71-80.

[7] Wu, L. X., Murphy, K., Karbhari, V. M., and Zhang, J. S., 2002, "Short-term effects of sea water on E-glass/vinylester composites," *Journal of Applied Polymer Science*, 84(14), pp. 2760-2767.

[8] Hale, J. M., and Gibson, A. G., 1998, "Coupon tests of fibre reinforced plastics at elevated temperatures in offshore processing environments," *Journal of Composite Materials*, 32(6), pp. 526-543.

[9] Mourad, A. H. I., Abdel-Magid, B. M., El-Maaddawy, T., and Grami, M. E., 2010, "Effect of Seawater and Warm Environment on Glass/Epoxy and Glass/Polyurethane Composites," *Applied Composite Materials*, 17(5), pp. 557-573.

[10] Radha, J. C., and Ranganathaiah, C., 2008, "Effect of hygrothermal aging on the diffusion of seawater in epoxy/glass composites studied by positron lifetime spectroscopy," *Polymer Composites*, 29(2), pp. 149-155.

[11] Puh, J. S., Wagner, P. A., Little, B. J., and Bradley, W. L., 1998, "The effect of biofouling on graphite/epoxy composites," *Journal of Composites Technology & Research*, 20(1), pp. 59-67.

[12] Davies, P., Pomies, F., and Carlsson, L. A., 1996, "Influence of water absorption on transverse tensile properties and shear fracture toughness of glass/polypropylene," *Journal of Composite Materials*, 30(9), pp. 1004-1019.

[13] Davies, P., Mazeas, F., and Casari, P., 2001, "Sea water aging of glass reinforced composites: Shear behaviour and damage modelling," *Journal of Composite Materials*, 35(15), pp. 1343-1372.

[14] Hammond, D. A., Amateau, M. F., and Queeney, R. A., 1993, "CAVITATION EROSION PERFORMANCE OF FIBER-REINFORCED COMPOSITES," *Journal of Composite Materials*, 27(16), pp. 1522-1544.

[15] Kahraman, R., 2005, "Effects of the aluminum filler content on moisture diffusion into epoxy adhesives in distilled water and sea water,"

Journal of Applied Polymer Science, 98(3), pp. 1165-1171.

[16] Siddaramaiah, Suresh, S. V., Atul, V. B., Srinivas, D., and Girish, S., 1999, "Effect of aggressive environments on composite properties," Journal of Applied Polymer Science, 73(5), pp. 795-799.

[17] Arsenault, T. J., Achuthan, A., Marzocca, P., Grappasonni, C., and Coppotelli, G., 2013, "Development of a FBG based distributed strain sensor system for wind turbine structural health monitoring," Smart Materials and Structures, 22(7), p. 11.

[18] Friebele, E. J., Askins, C. G., Putnam, M. A., Fosha, A. A., Florio, J., Donti, R. P., and Blosser, R. G., 1994, "DISTRIBUTED STRAIN SENSING WITH FIBER BRAGG GRATING ARRAYS EMBEDDED IN CRTM(TM) COMPOSITES," Electronics Letters, 30(21), pp. 1783-1784.

[19] Kim, S. W., Kang, W. R., Jeong, M. S., Lee, I., and Kwon, I. B., 2013, "Deflection estimation of a wind turbine blade using FBG sensors embedded in the blade bonding line," Smart Materials and Structures, 22(12), p. 11.

[20] 2013, "FBG Total Strain Sensor Thermal Considerations: Five Steps to Meaningful Strain Data," Micron Optics, Inc.

[21] 2008, "os3200 Strain Gage Installation Procedure," Micron Optics, Inc.

[22] 2009, "Non-metallic Optical Strain Gage: os3200," Micron Optics, Inc.

[23] 2009, "Fiber Bragg Grating: os1100," Micron Optics, Inc.

[24] Mandell, J. F., and Samborsky, D. D., 2011, "DOE/MSU Fatigue of Composite Materials Database," Montana State University Sandia National Laboratories